the only treatment available for patients with chronic HCV infections is combinational therapy with interferon (IFN) and ribavirin. The standard therapy is only effective for approximately 50% of patients with chronic HCV hepatitis [3]. Therefore, there is a great need for less complicated and more generally efficient therapeutics for HCV infection.

We and others reported that the synthetic siRNA and the siRNA-expressing adenovirus targeting 5′-UTR of HCV genome efficiently and specifically inhibited the HCV replication *in vitro* [4–6]. Other than humans, only chimpanzees can be productively infected by HCV. Together with ethical issues it has becomes increasingly difficult to access chimpanzees for experimental studies. The new world monkeys, tamarins and marmosets, undergo hepatitis upon infection with the GBV-B, which is most closely related to HCV. The significant similarity between HCV and GBV-B at the genomic and biochemical levels led to the proposal of the GBV-B/monkey system as a good surrogate model for hepatitis C [7,8]. Taking advantage of this non-human primate surrogate model, we investigated the feasibility of siRNA-mediated therapy against infectious diseases caused by pathogenic viruses.

## Materials and methods

*Preparation of siRNA.* The sequence of siRNA for GBV-B was cucguagaccguagcacau dTdT in the sense strand and augugcuacggucuacgagdTdT in the antisense strand which was designed to target the GBV-B RNA (Fig. 1). The sequence of control siRNA for experiments of Fig. 2A and B was uua ugc cga ucg cgu cac a dTdT in the sense strand and ugu gac gcg auc ggc aua a dTdT in the antisense strand which was designed to target beta-galactosidase RNA, and that for experiments of Figs. 3 and 4 was gct atg aaa cga tat ggg c dTdT in the sense strand and g ccc aua ucg uuu cau ugc dTdT in the antisense strand which was designed to target *firefly*-luciferase RNA. siRNA oligonucleotides were chemically synthesized and purified by reverse-phase high-performance liquid chromatography, while the unconjugated RNA oligonucleotides were purified by anion-exchange high-performance liquid chromatography. The sense and antisense strands were annealed at 95 °C for 1 min followed by slow cooling in RNAse free water. Positively charged liposomes containing cationic lipid analogue were synthesized at Nippon Shinyaku Co., as described previously [9]. To prepare CL-siRNA,

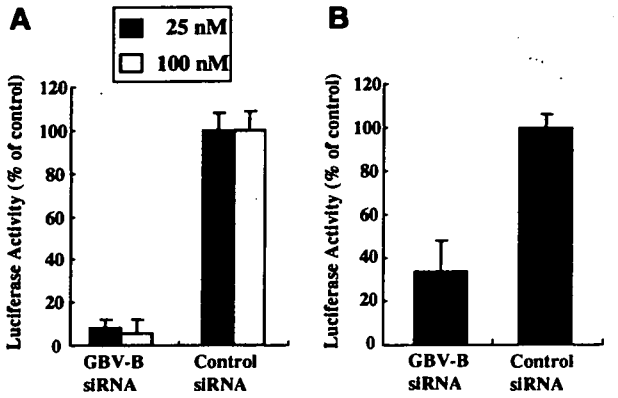


Fig. 2. Effects of the siRNA oligonucleotides on expression of GBV-B-reporter gene in culture cells. (A) and liver of mice (B).

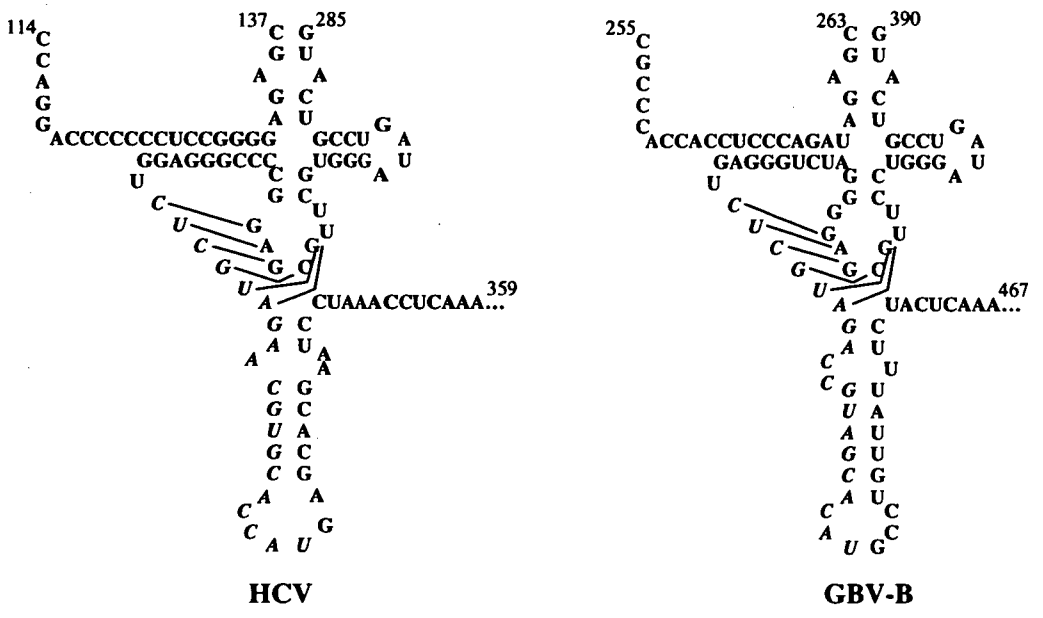


Sense sequence of siRNA

HCV : CUCGUAGAACGU(A)GCACAU

GBV-B : CUCGUAGACCGU A GCACAU

Fig. 1. Predicted secondary structure of the 5′-untranslated region around the target site (italic) in the HCV and GBV-B genome (nucleotide 114–137 and 285–359 of HCV, and 263–255 and 390–467 of GBV-B), and the sense sequences of siRNA.

annealed siRNA was added to the same volume of liposome solution with sonication. The ratio of oligonucleotide to LIC-101 was 1:16 (w/w).

*Cells culture and transfection.* The human embryonic kidney cell line, 293 T, was maintained in Dulbecco's modified minimal essential medium (Sigma, St. Louis, Missouri) supplemented with 10% fetal calf serum at 37 °C under 5% $CO_2$. Transfections of the siRNA oligonucleotides and the plasmids were performed in 24-well plates using Lipofectamine 2000 reagent (Invitrogen, Carlsbad, CA) as per the manufacturer's instructions. GBV-B-RNA-reporter gene vector, pGBV-B-Rluc, was used as a target, which expressed mRNA consisting of GBV-B 5′-untranslated region and upstream part of the core region (nucleotide 1–377) connected with upstream of *renilla* luciferase (RLuc) gene. Fifty nanograms of the pGBV-B-Rluc and 2 and 25 nM of siRNA were transiently transfected with 20 ng of *firefly* luciferase (FLuc)-expressing plasmid (pRL-RSV, Promega). The RLuc activity was adjusted by the FLuc activity, to normalize the transfection efficiency.

*Luciferase assays.* Luciferase activities were quantified with a luminometer (Lumat LB9501, Promega) using the Bright-Glo Luciferase Assay System (Promega). Assays were performed in triplicate and the results expressed as means ± SD as percentages of controls.

*Animals.* Male BALB/c or ICR mice, 9 weeks of age, were obtained from CLEA Japan and subject to a 2-week quarantine and acclimation period before use. Male juvenile common marmosets (*Callithrix jacchus*) were housed in individual cages at the Tsukuba Primate Medical Center. All animal studies were conducted in accordance with the protocols of experimental procedures which were approved by the Animal Welfare and Animal Care Committee of the National Institute of Biomedical Innovation and Tokyo Medical and Dental University.

*In vivo efficacy experiments in mice.* For the *in vivo* delivery of the siRNA to the liver of mice and monkeys, we used a novel cationic liposome that was synthesized by Nippon Shinyaku Co., Ltd. This cationic liposome was reported to be a good vehicle for the delivery of nucleic acid polymers and siRNAs to the liver when it was administered intravenously [9,10] or to the bladder by intravesical administration [11]. For the delivery of plasmid DNA to the liver of mice we used the hydrodynamic injection method in which a large volume of nucleotides solution was rapidly injected from tail vein [12]. *Three mice for each group were examined.* 5.0 mg/kg GBV-B or control CL-siRNA was administered as a regular intravenous injection from the tail vein in 0.2 ml 10% maltose over a period of 1–3 s. Three minutes later, the 50 μg of the pGBV-B-Rluc and 20 μg of pRL-RSV plasmids in a volume equivalent to 5% of the body weight were rapidly injected in 3–5 s into the mouse tail vein according to the hydrodynamic injection method. Phosphate buffer saline (PBS) was used as a carrier solution for injection. Successful injection was monitored when the conjunctiva of mouse became transiently anemic and confirmed by the luciferase activity in the liver.

In vivo efficacy experiments in monkeys. Negative control (n = 2; with or without control siRNA) and treatment group (n = 3; 1.0, 2.5 and 5.0 mg/kg of anti-GBV-B siRNA) were employed in this study. GBV-B-infectious serum obtained from a tamarin [8] was intrahepatically inoculated with the GBV-B RNA. The siRNA to GBV-B and control siRNA formulated by the cationic liposome, or just 10% maltose (sham) was administered by standard intravenous injection via the saphenous vein of the marmosets for three days. On the second day, the GBV-B infectious serum ($1.3 \times 10^9$ viral RNA copies/inoculum) was directly injected to the liver of five marmosets. Blood samples were periodically collected from the femoral vein of the monkeys under anesthetization. GBV-B RNA in plasma from the monkeys was quantified by a real-time, 5′ exonuclease PCR (TaqMan) assay using a primer-probe combination that recognized a portion of the GBV-B capsid gene as previously described [8]. The Platelet cell counts were performed at FALCO Biosystems, Co., Ltd.

*Measurement of IFNs in mice and monkeys.* The siRNA/cationic liposome was injected from tail vein of ICR mice or saphenous vein of the marmosets. Bood samples were taken 3 h after the injection. Mouse IFN-α levels were quantified by using sandwich ELISA kits for mouse IFNs (PBL Biomedical Laboratories, Biosource). Marmoset IFN-α and -γ levels were by using sandwich ELISA kits for human and rhesus macaque IFN, respectively (U-CyTech bioscience) according to the manufacture's instructions. Assays were performed in duplicate and the results expressed as means ± SD as percentages of controls.

## Results

We selected the siRNA-targeting site to the GBV-B genome from its 5′-UTR, the most conservative portion in both GBV-B and HCV genomes [13], to protect the siRNA from escape mutations of the virus [4]. The secondary structures of virus genome RNAs of HCV and GBV-B around the target site are very similar to each other, and the designed siRNA was different from the corresponding sequence of HCV by only two nucleotides (Fig. 1).

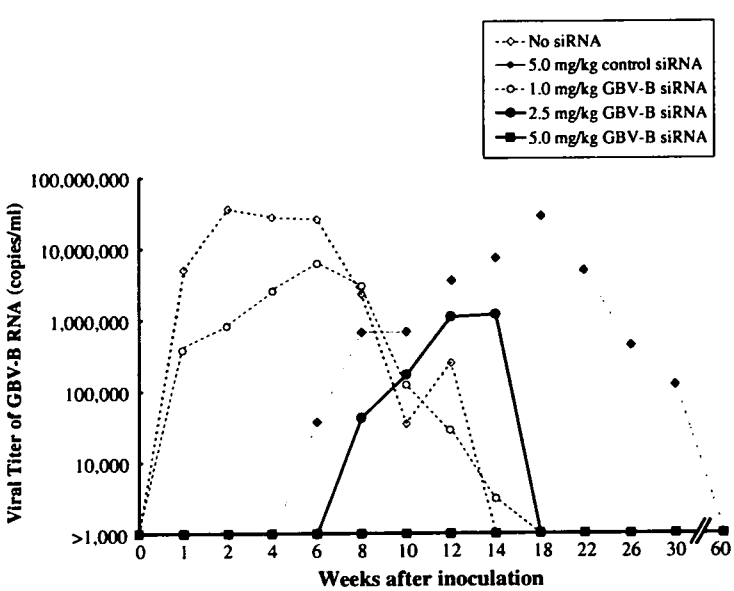


Fig. 3. Effect of the GBV-B siRNA/cationic liposome complex on replication of GBV-B in marmosets.

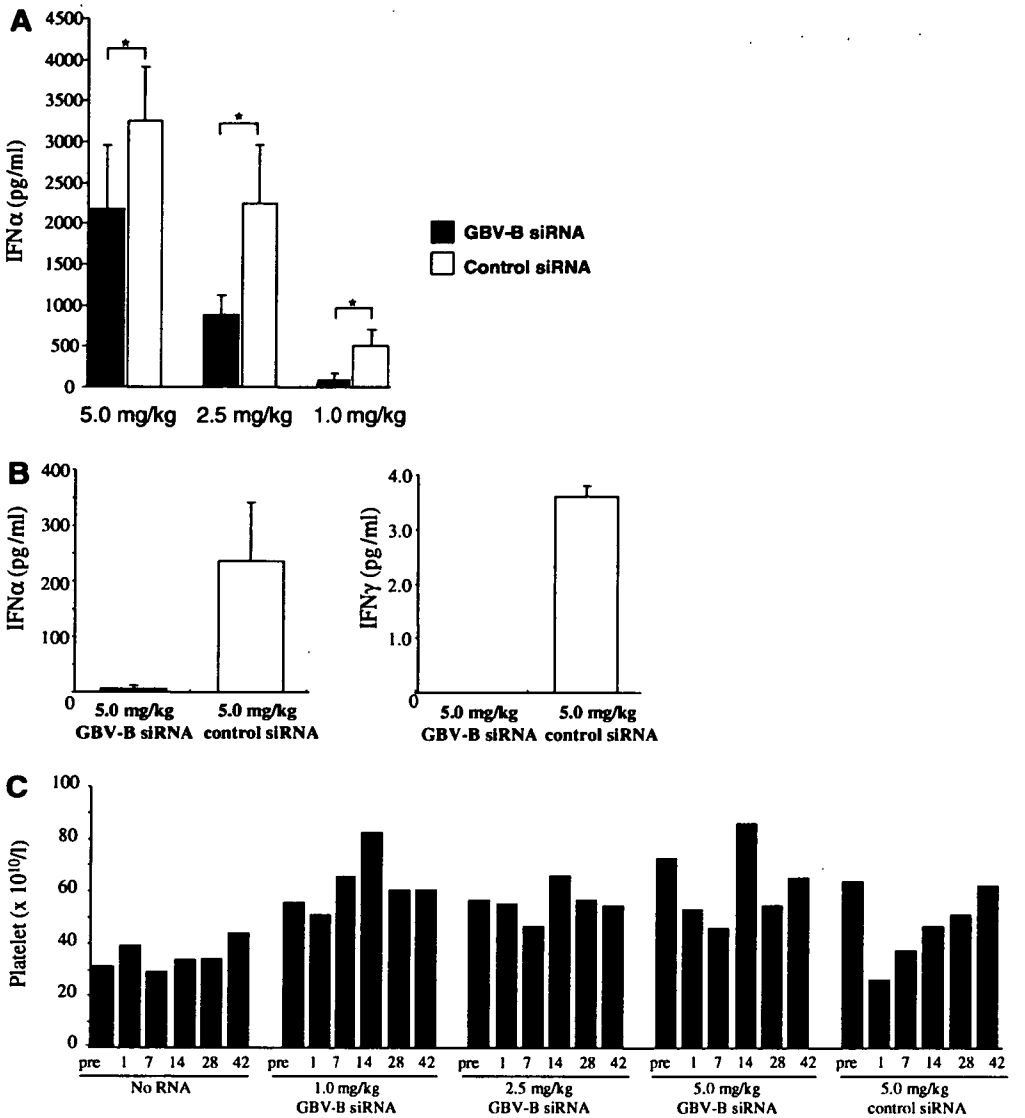


Fig. 4. Side effects of siRNA/cationic liposome complex. (A) Induction of IFN-α was evaluated by measuring mouse serum 3 h after intravenous injection of 1–5 mg/kg GVB-B or control siRNA/cationic liposome complex ($n = 3$). *<0.05 (Student $t$ test). (B) Induction of IFN-α and γ was evaluated by measuring marmoset serum 3 h after intravenous injection of 5 mg/kg GVB-B or control siRNA/cationic liposome complex), respectively ($n = 3$). (C) Peripheral blood platelet was counted in the five marmosets examined in the same experiment shown in Fig. 3.

*Effect of siRNA in vitro and in mice*

First, we confirmed the efficient cleavage of GBV-B RNA by the siRNA in 293 T cells. The cells were harvested at 24 h of transfection with pGBV-B-*R*luc, pRL-RSV and siRNA oligonucleotides, and internal luciferase activities were measured and ratio of RLuc versus FLuc value was calculated. More than 90% the *R*Luc activities were inhibited by expressing co-transfected siRNA (Fig. 2A). This result clearly indicated that GBV-B siRNA efficiently inhibited the expression of GBV-B RNA in culture cells.

Next, we investigated the *in vivo* effect of siRNA formulated in the cationic liposome on silencing the viral gene expression in the liver of mice. BALB/c mice were injected intravenously from the tail vein with GVB-B CL-siRNA followed by hydrodynamically injection of pGBV-B-*R*luc and pRL-RSV. We found that intravenously administered GBV-B CL-siRNA efficiently suppressed the expression of GBV-B genome in the liver of mice (Fig. 2B).

*Effect of siRNA on GBV-B replication in marmosets*

The 1.0, 2.5 and 5.0 mg/kg/day of siRNA to GBV-B, 5.0 mg/kg/day of control siRNA formulated by the cationic liposome, or just 10% maltose (sham) were administered by standard intravenous injections via the saphenous vein of the marmosets for three consecutive days. On the second day, GBV-B infectious serum

($1.3 \times 10^9$ viral RNA copies/inoculum) was directly injected to the liver. Before and after the inoculation, GBV-B RNA in the serum was quantified by a real-time, 5' exonuclease PCR. In a sham-administered marmoset, the viral RNA was transiently increased in plasma after infection and the viral load reached to the peak level ($3.6 \times 10^7$ copies/ml) (Fig. 3). It has been reported that GBV-B infection in marmosets as well as tamarins causes semi-acute viremia which generally ceases within 10–12 weeks post-infection [8,14,15]. This viral kinetics is consistent with the cases of HCV-infected human or chimpanzee, thus it appears to be in vivo characteristics of genus hepativirus where HCV and GBV-B belong to. Virological or immunological implication for the transient viremia is not fully addressed.

In contrast to sham-administered marmoset, we could find that the administration of CL-siRNA significantly delayed or suppressed the replication of GBV-B in a dose-dependent manner; the 5.0 mg/kg CL-siRNA completely suppressed the replication of GBV-B for more than 6 months after the infection (Fig. 3), even though the siRNA was administered only for the initial 3 days. Unexpectedly, the 5.0 mg/kg of control CL-siRNA was also able to delay the virus replication, while the peak level was comparable with that of the untreated monkey (Fig. 3).

*Induction of interferons*

We evaluated the induction of serum IFN-α by intravenous administration of the siRNA with cationic liposome in mice. IFN-α was induced by CL-siRNA but not by the cationic liposome nor siRNA oligonucleotide alone (data not shown). Induced IFN levels in the sera were dose-dependent and were significantly higher in mice with the *control CL-siRNA* than those with the *GBV-B CL-siRNA* (Fig. 4A).

An independent experiment using marmosets showed that single injection of 5.0 mg/kg control CL-siRNA substantially induced the serum interferon (IFN)-α and -γ, whereas the same dose of CL-siRNA induced a minimal level of IFN-α and no detectable level of IFN-γ (Fig. 4B).

In addition, a transient and mild decrease in peripheral blood platelets was more clearly observed in the marmoset treated with 5.0 mg/kg of control than 5.0 mg/kg of GBV-B CL-siRNA (Fig. 4C). There was no other remarkable abnormality related to siRNA administration in biochemical parameters indicating liver dysfunction which include alanine aminotransferase, aspartate aminotransferase, lactate dehydrogenase and albumin.

## Discussion

Many viruses produce some dsRNA as a byproduct of their replication [16], and RNAi serves as an important defense against viruses in plants [17]. Therefore, mammalian viruses have been expected to be a good therapeutic target of RNAi, and indeed, several animal viruses have been successfully inhibited to replicate *in vitro* [18]. Locally delivered siRNA have proven effective in abrogating infection from respiratory [19–22] and vaginal [23] viruses. Recently, systemically-delivered siRNA in mice has been successfully suppressed the expression of endogeous gene of the liver [24–26]. However, it remains to be ascertained if the RNAi-mediated gene therapy with systemically-delivered siRNA would be applicable to hepatitis virus in non-human primates. In this study, we examined if RNAi therapy could be effective toward infectious diseases by using a non-human primate surrogate model for hepatitis C. Administration into marmosets of CL-siRNA for GBV-B, which is most closely related to hepatitis C virus, repressed GBV-B replication in a dose-dependent manner. Our results suggest the feasibility of systemic administration of CL-siRNA as an antiviral strategy.

The 5.0 mg/kg GBV-B CL-siRNA dramatically inhibited the replication of GBV-B. However, control CL-siRNA also delayed the virus replication. Intravenous injection of siRNA formulated with liposomes was reported to stimulate mammalian immune system [26,27]. In relation to antiviral effect of IFNs, we therefore measured the serum IFN levels. Since the GBV-B siRNA/cationic liposome had less effect in IFN induction than the control but better antiviral effect than the control, it is possible that inhibition of the viral replication by the GBV-B siRNA/cationic liposome complex was at least in part caused by RNA interference. On the other side, it is also likely that IFN locally induced in the marmoset liver contributed the suppression of the viral replication. Because the induced level of mice serum IFN-α by GBV-B CL-siRNA was significant, although it was less than that by control CL-siRNA. Moreover, estimated IFNs level in marmoset serum was minimal but their actual levels might have been more, because the standard IFN in the ELISA was human or rhesus macaque IFN. Therefore, we considered that the antiviral effect of CL-siRNA was made by both RNA interference and induced IFNs.

In therapeutic application of siRNA to humans, general safety is a most important problem. The side effect of CL-siRNA to the liver is thought to consist of direct liver toxicity which is probably caused by its hydrophobic nature and its immuno-stimulatory effect [26–28]. Recently, Zimmermann et al. has reported that siRNA delivered systemically in a cationic liposome, stable nucleic acid lipid particles (SNALP), inhibited endogenous gene expression in the liver of the cynomolgus monkeys, which supports our notion concerning the therapeutic potential of systemically injected siRNA in primates. Although they made excellent chemical modifications to siRNA oligonucleotides to reduce IFN induction, their siRNA complex produced a considerable liver damage with a marked increase of transaminases at the dose (2.5 mg/kg) of maximal suppression effect. This indicated that the therapeutic window of their siRNA complex is overlapped with its toxic window. In contrast, our CL-siRNA induced much less liver damage, since even the 5.0 mg/kg of our CL-siRNA did not show a marked liver damage, but induced a sub-

stantial immune responses. A number of recent studies revealed that siRNA/cationic liposome complex has an immunological effects of siRNAs including the induction of proinflammatory cytokines and type I IFNs (IFN-α and IFN-β) through activation of RNA-sensing immunoreceptors including three members of the Toll-like receptor (TLR) family (TLR3, TLR7 and TLR8) [29]. Detection of siRNA molecules could trigger antiviral innate defense mechanisms including the induction of type I IFNs. In fact, double strand RNA molecule, poly I/C, was reported to eliminate the virus in GBV-B-infected tamarin hepatocytes by activating TLR3 [30,31]. These knowledges lead us to postulate that it is one of sophisticated strategy for siRNA to inhibit hepatitis virus to use this immuno-stimulatory side effect as an antiviral innate defense, only if the systemic side effects are tolerable.

## Acknowledgments

We thank members of Corporation for Production and Research of Laboratory Primates for their technical support, N. Enomoto (Yamanashi University) for the invaluable suggestions and encouragements, and S. Arold (CNRS, France) for critical reviewing of the manuscript. RNAs and cationic liposome were supplied by Nippon Shinyaku Co., Ltd. This work was supported by Grants from the Ministry of Education, Science and Culture, Japan (#18390215, T.Y. and H.A.) and from the Ministry of Health, Labor and Welfare, Japan (#2212065, T.Y; #17200101, H.A.).

## References

[1] G.J. Hannon, RNA interference, Nature 418 (2002) 244–251.
[2] W.R. Kim, The burden of hepatitis C in the United States, Hepatology 36 (2002) S30–S34.
[3] J.M. Mchutchison, Hepatitis C advances in antiviral therapy: what is accepted treatment now? J. Gastroenterol. Hepatol. 17 (2002) 431–441.
[4] T. Yokota, N. Sakamoto, N. Enomto, H. Tanabe, M. Maekawa, M. Miyagishi, K. Taira, M. Watanabe, H. Mizusawa, Inhibition of intracellular hepatitis C Virus replication by synthetic and vector-derived small interfering RNAs, EMBO Rep. 4 (2003) 602–608.
[5] M.Y. Seo, S. Abrignani, M. Houghton, J.H. Han, Small interfering RNA-mediated inhibition of hepatitis C virus replication in the human hepatoma cell line Huh-7, J. Virol. 77 (2003) 810–812.
[6] M. Korf, D. Jarczak, C. Beger, M.P. Manns, M. Kruger, Inhibition of hepatitis C virus translation and subgenomic replication by siRNAs directed against highly conserved HCV sequence and cellular HCV cofactors, J. Hepatol. 43 (2005) 225–234.
[7] A. Martin, F. Bodola, D.V. Sangar, K. Goettge, V. Popov, R. Rijnbrand, R.E. Lanford, S.M. Lemon, Chronic hepatitis associated with GB virus B persistence in a tamarin after intrahepatic inoculation of synthetic viral RNA, Proc. Natl. Acad. Sci. USA 100 (2003) 9962–9967.
[8] K. Ishii, S. Iijima, N. Kimura, Y.-J. Lee, N. Ageyama, S. Yagi, K. Yamaguchi, N. Maki, K. Mori, S. Yoshizaki, S. Machida, T. Suzuki, N. Iwata, T. Sata, K. Terao, T. Miyamura, H. Akari, GBV-B as a pleiotropic virus: distribution of GBV-B in extrahepatic tissues in vivo, Microb. Infect. 9 (2007) 515–521.
[9] K. Hirabayashi, J. Yano, T. Inoue, T. Yamaguchi, K. Tanigawara, G.E. Smyth, K. Ishiyama, T. Ohgi, K. Kimura, T. Irimura, Inhibition of cancer cell growth by polyinosinic-polycytidylic acid/cationic liposome complex: a new biological activity, Cancer Res. 59 (1999) 4325–4333.
[10] J. Yano, K. Hirabayashi, S. Nakagawa, T. Yamaguchi, M. Nogawa, I. Kashimori, H. Naito, H. Kitagawa, K. Ishiyama, T. Ohgi, T. Irimura, Antitumor activity of small interfering RNA/cationic liposome complex in mouse models of cancer, Clin. Cancer Res. 10 (2004) 7721–7726.
[11] M. Nogawa, T. Yuasa, S. Kimura, M. Tanaka, J. Kuroda, K. Sato, A. Yokota, M. Koizumi, T. Maekawa, Intravesical administration of small interfering RNA targeting PLK-1 successfully prevents the growth of bladder cancer, J. Clin. Invest. 115 (2005) 978–985.
[12] F. Liu, Y.K. Song, D. Liu, Hydrodynamics-based transfection in animals by systemic administration of plasmid DNA, Gene Ther. 6 (1999) 1258–1266.
[13] A.A. Kolylhalov, K. Mihalik, S.M. Feinstone, C.M. Rice, Hepatitis C virus-encoded enzymatic activities and conserved RNA elements in the 3' nontranslated region are essential for virus replication in vivo, J. Virol. 74 (2000) 2046–2051.
[14] J.R. Jacob, K.C. Lin, B.C. Tennant, K.G. Masnfield, GB virus B infection of the common marmoset (*Callithrix jacchus*) and associated liver pathology, J. Gen. Virol. 85 (2004) 2525–2533.
[15] R.E. Lanford, D. Chavez, L. Notvall, K.M. Brasky, Comparison of tamarins and marmosets as hosts for GBV-B infections and the effect of immunosuppression on duration of viremia, Virology 311 (2003) 72–80.
[16] B.L. Jacobs, J.O. Langland, When two strands are better than one: the mediators and modulators of the cellular responses to double-stranded RNA, Virology 219 (1996) 339–349.
[17] M.T. Mcmanus, Small RNAs and immunity, Immunity 21 (2004) 747–756.
[18] J.N. Leonard, D.V. Shaffer, Antiviral RNAi therapy: emerging approaches for hitting a moving target, Gene Ther. 13 (2006) 532–540.
[19] V. Bitko, A. Musiyenko, O. Shulyayeva, S. Barik, Inhibition of respiratory viruses by nasally administered siRNA, Nat. Med. 11 (2005) 50–55.
[20] W. Zhang, H. Yang, X. Kong, S. Mohapatra, H. San Juan-Vergara, G. Hellermann, S. Behera, R. Singam, R.F. Lockey, S.S. Mohapatra, Inhibition of respiratory syncytial virus infection with intranasal siRNA nanoparticles targeting the viral NS1 gene, Nat. Med. 11 (2005) 56–62.
[21] B.J. Li, Q. Tang, D. Cheng, C. Qin, F.Y. Xie, Q. Wei, J. Xu, Y. Liu, B.J. Zheng, M.C. Woodle, N. Zhong, P.Y. Lu, Using siRNA in prophylactic and therapeutic regimens against SARS coronavirus in Rhesus macaque, Nat. Med. 11 (2005) 944–9451.
[22] S.M. Tompkins, C.Y. Lo, T.M. Tumpey, S.L. Epstein, Protection against lethal influenza virus challenge by RNA interference in vivo, Proc. Natl. Acad. Sci. USA 101 (2004) 8682–8686.
[23] D. Palliser, D. Chowdhury, Q.Y. Wang, S.J. Lee, R.T. Bronson, D.M. Knipe, J. Lieberman, An siRNA-based microbicide protects mice from lethal herpes simplex virus 2 infection, Nature 439 (2006) 89–94.
[24] J. Soutschek, A. Akinc, B. Bramlage, K. Charisse, R. Constien, M. Donoghue, S. Elbashir, A. Geick, P. Hadwiger, J. Harborth, M. John, V. Kesavan, G. Lavine, R.K. Pandey, T. Racie, K.G. Rajeev, I. Rohl, I. Toudjarska, G. Wang, S. Wuschko, D. Bumcrot, V. Koteliansky, S. Limmer, M. Manoharan, H.P. Vornlocher, M. Manoharan, H.P. Vornlocher, Therapeutic silencing of an endogenous gene by systemic administration of modified siRNAs, Nature 432 (2004) 173–178.
[25] E. Song, P. Zhu, S.K. Lee, D. Chowdhury, D.M. Dykxhoorn, Y. Feng, D. Palliser, D.B. Weiner, P. Shankar, W.A. Marasco, J. Lieberman, Antibody mediated in vivo delivery of small interfering RNAs via cell-surface receptors, Nat. Biotechnol. 23 (2005) 709–717.

[26] D.V. Morrissey, J.A. Lockridge, L. Shaw, K. Blanchard, K. Jensen, W. Breen, K. Hartsough, L. Machemer, S. Radka, V. Jadhav, N. Vaish, S. Zinnen, C. Vargeese, K. Bowman, C.S. Shaffer, L.B. Jeffs, A. Judge, I. Maclachlan, B. Polisky, Potent and persistent in vivo anti-HBV activity of chemically modified siRNAs, Nat. Biotechnol. 23 (2005) 1002–1007.

[27] A.D. Judge, V. Sood, J.R. Shaw, D. Fang, K. Mcclintock, I. Maclachlan, Sequence-dependent stimulation of the mammalian innate immune response by synthetic siRNA, Nat. Biotechnol. 23 (2005) 457–462.

[28] T.S. Zimmeemamm, A.C. Lee, A. Akinc, B. Bramlage, D. Bumcrot, M.N. Fedoruk, J. Harborth, J.A. Heyes, L.B. Jeffs, M. John, A.D. Judge, K. Lam, K. McClintock, L.V. Nechev, L.R. Palmer, T. Racie, I. Rohl, S. Seiffert, S. Shanmugam, V. Sood, J. Soutschek, I. Toudjarska, A.J. Wheat, E. Yaworski, W. Zedalis, V. Koteliansky, M. Manoharan, H.P. Vornloche, I. MacLachlan, RNAi-mediated gene silencing in non-human primates, Nature 441 (2006) 111–114.

[29] M. Schlee, V. Hornung, G. Hartmann, siRNA and isRNA: two edges of one sword, Mol. Ther. 14 (2006) 463–470.

[30] R.E. Lanford, D. Chavez, B. Guerra, J.Y.N. Lau, Z. Hong, K.M. Brasky, B. Beames, Ribavirin induces error-prone replication of GB virus B in primary tamarin hepatocytes, J. Virol. 75 (2001) 8074–8081.

[31] K. Li, Z. Chen, N. Kato, M. Gale Jr., S.M. Lemon, Distinct poly(I-C) and virus-activated signaling pathways leading to interferon-beta production in hepatocytes, J. Biol. Chem. 280 (2005) 16739–16747.

ELSEVIER

INSTITUT PASTEUR

Microbes and Infection 9 (2007) 515–521

www.elsevier.com/locate/micinf

Original article

# GBV-B as a pleiotropic virus: distribution of GBV-B in extrahepatic tissues *in vivo*

Koji Ishii [a], Sayuki Iijima [b], Nobuyuki Kimura [b], Young-Jung Lee [b], Naohide Ageyama [b], Shintaro Yagi [d,1], Kenjiro Yamaguchi [d], Noboru Maki [d], Ken-ichi Mori [d], Sayaka Yoshizaki [a], Sanae Machida [a,e], Tetsuro Suzuki [a], Naoko Iwata [c], Tetsutaro Sata [c], Keiji Terao [b], Tatsuo Miyamura [a], Hirofumi Akari [b,*]

[a] *Department of Virology II, National Institute of Infectious Diseases, 1-23-1 Toyama, Shinjuku-ku, Tokyo 162-8640, Japan*
[b] *Laboratory of Disease Control, Tsukuba Primate Research Center, National Institute of Biomedical Innovation, 1-1 Hachimandai, Tsukuba, Ibaraki 305-0843, Japan*
[c] *Department of Pathology, National Institute of Infectious Diseases, 1-23-1 Toyama, Shinjuku-ku, Tokyo 162-8640, Japan*
[d] *Advanced Life Science Institute, Wako, Saitama 351-0112, Japan*
[e] *Department of Microbiology, Saitama Medical School, Moroyama-Cho, Iruma-Gun, Saitama 350-0495, Japan*

Received 25 August 2006; accepted 16 January 2007
Available online 27 January 2007

**Abstract**

GB virus B (GBV-B) infection of New World monkeys is considered to be a useful surrogate model for hepatitis C virus (HCV) infection. GBV-B replicates in the liver and induces acute resolving hepatitis but little is known whether the other organs could be permissive for the virus. We investigated the viral tropism of GBV-B in tamarins in the acute stage of viral infection and found that the viral genomic RNA could be detected in a variety of tissues. Notably, a GBV-B-infected tamarin with marked acute viremia scarcely showed a sign of hepatitis, due to preferential infection in lymphoid tissues such as lymph nodes and spleen. These results indicate that GBV-B as well as HCV is a pleiotropic virus *in vivo*.


*Keywords:* GB virus B; Hepatitis C virus; Tamarin; Surrogate model

## 1. Introduction

Over 100 million people worldwide are carriers of hepatitis C virus (HCV) and the viral infection is a significant cause of human morbidity and mortality; chronic HCV infection in many cases will lead to liver cirrhosis and hepatocellular carcinoma. Furthermore, HCV infection manifests a variety of extrahepatic, at least in part due to the extrahepatic tropisms of HCV, particularly lymphotropism diseases (for review see [1]).

Other than humans, only chimpanzees that are endangered as species can be productively infected by HCV. Together with ethical issues regarding animal experiments, it has becomes increasingly difficult to access chimpanzees for experimental studies. Tamarins (*Saguinus* species), one of the new world monkeys, develop acute, self-limited hepatitis upon infection with the GB virus B (GBV-B), which is most closely related to HCV [2–4]. Although the acute nature of GBV-B infection in tamarins has been distinguished this hepatitis from HCV infection in humans, recent studies demonstrated that tamarins could be persistently infected by GBV-B and developed chronic hepatitis [5,6]. Therefore, the GBV-B infection of tamarins is proposed as a good surrogate model for hepatitis C. While GBV-B appeared to infect liver, comprehensive documentation of the *in vivo* tropism of GBV-B has not been

* Corresponding author. Tel.: +81 29 837 2121; fax: +81 29 837 0218.
*E-mail address:* akari@nibio.go.jp (H. Akari).
[1] Present address: Laboratory of Cellular Biochemistry, Department of Animal Resource Sciences, Graduate School of Agricultural and Life Sciences, The University of Tokyo, Tokyo, Japan.

1286-4579/$ - see front matter © 2007 Elsevier Masson SAS. All rights reserved.
doi:10.1016/j.micinf.2007.01.010

reported yet. A previous report that GBV-B RNA was observed in peripheral blood mononuclear cells (PBMCs) from a GBV-B-infected marmoset [7] suggests that GBV-B may be lymphotropic as well as HCV. Considering the close similarity between HCV and GBV-B, we examined the viral distribution and tropism in tamarins in the acute phase of the viral infection.

## 2. Materials and methods

### 2.1. Animals

Adult white-lipped and Red-handed tamarins (*Saguinus labiatus* and *Saguinus midas*, respectively) were housed in individual cages at the Tsukuba Primate Research Center. All animal studies were conducted in accordance with the protocols of experimental procedures that were approved by the Animal Welfare and Animal Care Committees of the National Institute of Biomedical Innovation and National Institute of Infectious Diseases. The details of tamarins used in this study were summarized in Table 1.

### 2.2. GBV-B infection in tamarins

GBV-B RNA was transcribed *in vitro* with T7 RNA polymerase (Promega, Madison, WI) from 10 μg of *Xho*I-digested pGBB [2] that harbors infectious cDNA for GBV-B (kind gift of Dr. J. Bukh, National Institutes of Health, USA). The integrity of the RNA was checked by electrophoresis through an agarose gel stained with ethidium bromide. Each transcription mixture (400 μg of GBV-B RNA) was diluted with 400 μl of ice-cold water and then immediately frozen on dry ice and stored at −80 °C. Transcription mixtures were injected into each tamarin intrahepatically. For transmission of GBV-B, animals were infected intrahepatically with 100 μl of GBV-B infectious plasma containing $8 \times 10^8$ genome equivalents (GE) of the viral RNA. Blood samples were periodically collected from the monkeys from femoral vein under anesthetization and were tested for plasma ALT level.

### 2.3. Quantification of GBV-B genomic RNA

GBV-B-infected tamarins were euthanized and perfused with saline thoroughly before the collection of specimens including plasma, PBMCs and a variety of tissues (esophagus, stomach, duodenum, jejunum, ileum, cecum, colon, rectum, liver, pancreas, submandibular gland, trachea, lung, bone marrow, thymus, spleen, submandibular lymph nodes, axillary lymph nodes, intestinal lymph nodes, mesenteric lymph nodes, inguinal lymph nodes, tonsil, heart, kidney, adrenal gland, bladder, brain, spinal cord, testis, uterus and ovary). GBV-B RNA from these specimens was quantified by a real-time, 5′ exonuclease PCR (TaqMan) assay using a primer-probe combination that recognized a portion of the GBV-B capsid gene. The primers 558F [5′AACGAGCAAAGCGCAAAGTC] and 626R [5′CATCATGGATACCAGCAATTTTGT] and probe 579P [5′6FAM-AGCGCGATGCTCGGCCTCGTATAMRA] [8] were obtained from PE Biosystems. The primers were used at 15 pmol/50 μl reaction, and the probe was used at 10 pmol/50 μl reaction. Synthesized GBV-B RNA was used as a reference standard of GBV-positive plasma. PBMCs were isolated from whole blood by density-gradient centrifugation. Approximately 10 mg of tissues were removed under sterile conditions and immediately homogenized in 1 ml of TRIzol (Invitrogen, Carlsbad, CA) to extract RNA. We set our lowest detection cutoff at $10^2$ GE per ml. All the specimens were evaluated in duplicates and the averages were shown.

Table 1
Summary of the results of GBV-B RNA levels in the tissues of the virus-infected tamarins

| | | Tm3 | Tm4 | Tm5 | Tm6 |
|---|---|---|---|---|---|
| Animals | | *S. labiatus* | *S. midas* | *S. labiatus* | *S. midas* |
| Sex | | Female | Female | Male | Female |
| GBV-B inoculum | | Plasma | Plasma | RNA | RNA |
| Weeks at necropsy | | 4 | 4 | 3 | ND[a] |
| ALT | | 321 | 522 | 38 | 554 |
| Viral loads in: | | | | | |
| Blood | Plasma | $3.8 \times 10^8$ | $5.9 \times 10^8$ | $1.3 \times 10^{10}$ | $2.8 \times 10^9$ |
| | PBMC | 270 | 1630 | 35650 | ND |
| Spleen | | (−)[b] | 540 | 5980 | ND |
| Lymph nodes | Inguinal | (−) | (−) | 3090 | ND |
| | Intestinal | (−) | (−) | 640 | ND |
| Liver | | 70080 | 33480 | 16080 | ND |
| Kidney | | (−) | (−) | 380 | ND |
| Testis | | | | 600 | ND |
| Ovary | | 1290 | 150 | | ND |
| Bone marrow | | 120 | (−) | 750 | ND |

Viral loads in each tissues were presented as GE/mg except for plasma (GE/ml) and PBMC (GE/$10^6$ cells). Data for Tm6 were obtained at week 4.
[a] ND: not done.
[b] (−): undetectable.

### 2.4. Detection of anti-GBV-B core and NS3 antibodies by ELISA

The TrpE-core (aa 1 to 132) fusion protein and TrpE-NS3 (aa 1135 to 1378) fusion protein, representing a portion of NS3 identified as being immunogenic in infected animals [9], was expressed in *Escherichia coli* [10] to serve as an antigen to generate polyclonal rabbit antisera. Tamarin sera were tested for the presence of antibodies to GBV-B core and NS3 by ELISA as described previously [8].

### 2.5. Cloning of entire GBV-B genome from plasma, liver and PBMCs of infected tamarins

GBV-B RNA was isolated from plasma, liver and PBMCs as described above. GBV-B cDNA was synthesized using SuperScript reverse transcriptase II (Invitrogen) with GB-5145R primer (5′-GCG AGT GCG GCT GTC CCA GAA GTA TTG ACT-3′) or GB-9051R primer (5′-AAT TTG GGG GTT CAG CTG ATG GCT AAT CCA-3′). After RNase H (Invitrogen) treatment at 42 °C, a cDNA mixture was subjected to PCR with LA-taq DNA polymerase (TaKaRa), GB-5145R primer and GB-35S primer (5′-ACC ACA AAC ACT CCA GTT TGT TAC ACT CCG CTA GG-3′) or GB-9051R primer and GB-3999S primer (5′-CGT ACG GCG TGA ATC CAA ATT GCT ATT TTA-3′) for 30 cycles of denaturation at 94 °C for 20 s and extension at 68 °C for 5 min. PCR products were purified from the gel using a QIA-quick gel kit (Qiagen), and then cloned into pGEM-T Easy vector (Promega). Four clones of each fragment were determined using a CEQ-2000XL analysis system with a DTCS quick start kit and GBV-B specific primers according to the manufacturer's instructions. Sequence data were analyzed on Macintosh computers with the Sequencer (Gene Code Corp.) and MacVector (Accelrys) software packages.

### 2.6. Synthesis of positive and negative standard RNAs for RT–PCR controls

Recombinant positive and negative strand RNAs were generated from pGBB containing 3′ sequences of GBV-B. Positions 8569–9359 were amplified and inserted into pGEM-T easy vector. Clones were selected for sense and antisense orientation of the insert corresponding to positive and negative strands, respectively. Ten micrograms of the selected plasmids were linearized using *Pst*I and positive- and negative-strand RNAs were synthesized by transcription from the upstream T7 RNA polymerase promoter by Ambion MEGAscript T7 kit (Ambion, Austin, TX).

### 2.7. Detection of strand-specific viral RNA by tagging PCR system

One microgram of total RNA obtained from tissues or cells was subjected to RT–PCR. cDNAs were synthesized using Superscript III first strand synthesis system (Invitrogen). In order to overcome the detection of falsely primed cDNA products and make the PCR system strand-specific, additional nucleotides (TCATGGTGGCGAATAA) were added to the 5′ end of the reverse transcription primer (5′-TCATGGTGGC GAATAATTGGATTAGCCATCAGCTGAACC-3′), forming a "tag" (underlined) [11,12]. This "tag" sequence was neither complementary nor homologous to any part of the GBV-B genome. PCR amplification of a tagged cDNA was performed using only the tag portion of the cDNA primer (5′-TCATGG TGGCGAATAA-3′) as one of the primers and a GBV-B specific oligonucleotide for the opposing primer (5′-CTTGGTAC TACGCTCTGCACA-3′, positions 9339–9359). For the first round of PCR using 2 µl of cDNA in a final volume of 25 µl, the reactions were performed using a TaKaRa PCR kit (TaKaRa) with following conditions; a 20 s and 94 °C denaturation step followed by 20 s and 55 °C annealing and 2 min and 72 °C extension steps. After 30 cycles of first round amplification, 2 µl of reaction samples were subjected to 30 cycles of nested PCR using 5′-TTTTAGGGCAGCGGCAACAG-3′ (positions 9105–9124) and 5′-CACACAGCCAGGACTCCTCA-3′ (positions 9260–9279) as primers.

### 2.8. Histopathology

Five tamarin livers were used in this study. Of these, three livers were from GBV-B-infected tamarins (Table 1), and two were from uninfected tamarins. Liver samples obtained by necropsy were fixed with 4% paraformaldehyde, embedded in paraffin, and cut into 4 µm thick-sections. Deparaffinized sections were stained with hematoxylin and eosin (H&E) for histopathological analyses. To investigate apoptotic cells in the livers, we also examined both DNA fragmentation and immunohistochemistry for an active form of caspase-3. To diminish autofluorescence mainly caused by lipofuscin, sections were pre-stained with 1% Sudan black B. DNA fragmentation was evaluated by a TUNEL assay with an ApopTag Direct *In Situ* Apoptosis Detection Kit (Chemicon International, Temecula, CA) according to the manufacturer's instructions. Briefly, the specimens were digested with a solution of proteinase K (20 µg/ml) in PBS for 5 min and then incubated with terminal deoxynucleotidyl transferase (TdT) and fluorescein-labeled nucleotides (ApopTag Direct) in a humid atmosphere at 37 °C for 1 h. Specimens were viewed with a BX-FLA fluorescence microscope (Olympus, Tokyo, Japan). To control for nonspecific incorporation of nucleotides and nonspecific binding of TdT, cells were treated with proteinase K as usual, but staining was performed in the absence of active TdT. This served as a negative control. In parallel, immunohistochemistry for an active form of caspase-3 was examined by using an FITC-conjugated monoclonal antibody against the active caspase-3 (C92-605; BD Pharmingen, San Jose, CA) in order to confirm the degree of apoptotic cells detected by TUNEL staining. Sections were deparaffinized followed by autoclaving for 5 min at 121 °C, and then incubated free floating in the primary antibody solution overnight at 4 °C. Following brief washes, sections were then incubated with DAPI (1:800; Santa Cruz Biotechnology, Santa Cruz, CA) for 1 h at room temperature. These sections were examined with a Digital Eclipse C1 confocal microscope (Nikon, Japan).

## 3. Results

### 3.1. GBV-B infection in tamarins

Firstly, two tamarins were intrahepatically inoculated with RNA transcripts from GBV-B infectious molecular clone pGBB (Fig. 1). Both monkeys showed viremia at 2 weeks post inoculation; peak viral titers in plasma reached up to $10^9$ GE/ml and both monkeys developed hepatitis with dramatically elevated plasma ALT levels. The viremia was maintained up to 8 weeks, followed by rapid decline in parallel with the resolution of the ALT abnormalities. Within 6–8 weeks of the inoculation, the development of antibodies reactive with the viral core and NS3 proteins was observed (Fig. 1). Multiple plasma samples collected at later time points contained no detectable viral RNA and showed no ALT abnormalities; however, antibodies against GBV-B core and NS3 proteins were maintained at relatively high levels at least until 28 weeks after inoculation (Fig. 1). These results confirmed that inoculation of GBV-B viral RNA caused acute hepatitis in parallel with typical viremia in tamarins.

Next, in order to examine the tissue tropism of GBV-B *in vivo*, four tamarins were inoculated intrahepatically with week 2 plasma of tamarin Tm1 containing $8 \times 10^8$ GE of GBV-B (Tm3 and Tm4) or synthetic GBV-B RNA as described above (Tm5 and Tm6). These tamarins developed a typical acute infection that were marked by high levels of viremia, indicating that inoculation of either viral RNA or plasma of the infected tamarin resulted in comparable outcome (Fig. 2). It is noteworthy that in Tm5 the plasma ALT level was scarcely elevated in contrast with other three tamarins during the acute period of GBV-B infection, although this tamarin developed highest viremia ($1.3 \times 10^{10}$ GE/ml).

### 3.2. Histopathological analyses of GBV-B infection

Histopathological analyses in Tm3 and Tm4 livers showed inflammatory responses including inflammatory cell invasions around central and/or portal veins and hemorrhages, hepatocytic degenerations, and disruptions of sinusoids (Fig. 3A,B,E,F). Although there were only minimal pathological changes, hepatocytic degenerations and dilation of sinusoids were also found in the Tm5 liver (Fig. 3C and G) in contrast to uninfected tamarins (Fig. 3D and H, data not shown). To further evaluate the levels of apoptotic hepatocytes in these monkeys, we employed two different methods, detecting fragmented DNA (TUNEL assay) and an active form of caspase-3 as previously described [13]. It was found that substantial numbers of fragmented DNA-positive cells were observed in the Tm3 and Tm4 livers while much less in the Tm5 liver (Fig. 3I–K). Consistent results were obtained when the active form of caspase-3 was stained (Fig. 3M–O). On the other hand, we found neither DNA fragmentation nor caspase-3 activation in uninfected tamarin livers (Fig. 3L and P, data not shown). The minimal levels of pathological changes in the Tm5 liver were well correlated with a lower level of plasma ALT in Tm5 (Fig. 2, Table 1).

### 3.3. Tissue distribution of GBV-B

The results described above suggested the possibility that the substantial levels of viral replication occurred in other tissues rather than in the liver of Tm5. To ascertain the possibility, we euthanized three tamarins (Tm3, Tm4 and Tm5) and the viral levels in a variety of tissues were compared. Table 1 summarizes the data obtained in this experiment. It is reasonable to consider that GBV-B replicated in the liver accounts for majority of the viral load *in vivo*. However,

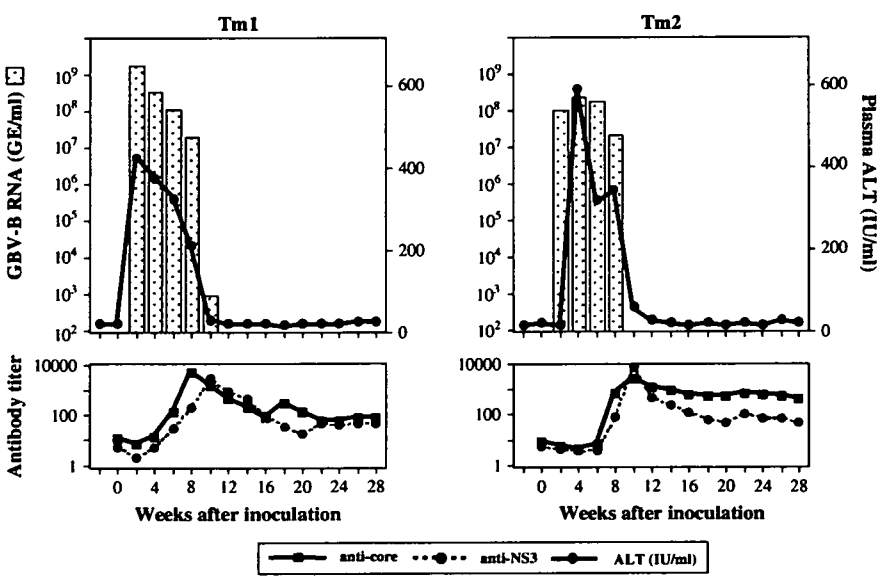


Fig. 1. Course of GBV-B infection in tamarins Tm1 and Tm2. Synthesized infectious RNA transcript of GBV-B from a pGBB molecular clone was inoculated into each tamarin intrahepatically. Plasma samples were collected from each tamarin at 2-week intervals post inoculation. The viral RNA copies, ALT levels, and titers of anti-viral antibodies (anti-core and anti-NS3) in the plasma samples until 28 weeks after inoculation were shown.

substantial levels of GBV-B RNA were detected not only in the liver but also in a variety of extrahepatic tissues such as hematolymphoid and genital tissues, suggesting that GBV-B may infect and replicate in these organs. Notably, the viral RNA levels of Tm5 were much greater in the lymphoid tissues but lower in the liver as compared with those of other two tamarins, indicating that the highest plasma viral load in Tm5 derived from extrahepatic tissues, mainly hematolymphoid tissues. We could not detect GBV-B RNA from other tissues tested (data not shown). From these results, we concluded that the preferential distribution of GBV-B in the extrahepatic tissues rather than in the liver of Tm5 may attribute to the highest plasma viral load in spite of the mild disorder and the lower viral load in the liver.

In addition, the unique viral distribution implied that the GBV-B disseminated in Tm5 might acquire novel tissue tropism as a result of genomic mutation. To ascertain the possibility, we amplified the entire viral genomes by RT–PCR from the liver, PBMCs and plasma collected from Tm5 at euthanasia and compared with the original nucleotide sequence. The sequences determined were completely identical to the original sequence of GBV-B (data not shown), indicating that the sequence heterogeneity of GBV-B was not responsible for the different tropism observed in Tm5 and thus GBV-B intrinsically exhibits pleiotropism in a host-dependent manner.

### *3.4. Detection of strand-specific viral RNA in the tamarin tissues*

To confirm that the virus was actually replicated in the tissues other than the liver, we sought to deferentially determine negative-strand viral RNA which is shown to be a viral replication intermediate in case of HCV. We thus newly developed an assay system for detecting replication intermediate of GBV-B.

To determine the sensitivity of this method, synthetic positive- and negative-strand GBV-B transcripts (ranging from $10^8$ to $10^0$ copies of GBV-B) in 100-fold serial dilutions were subjected to RT–PCR. As shown in Fig. 4A, at least 100 copies of GBV-B negative-strand RNA could be detected by this method. When the primer for cDNA synthesis was omitted, no PCR products were obtained (Fig. 4A, negative control), indicating that the PCR signals were derived specifically from the GBV-B negative-strand RNA. In the presence of $10^8$ copies of positive-strand HCV RNA, false positive PCR signals appeared (Fig. 4A). We then analyzed the samples from liver, spleen, pancreas, stomach and PBMCs from Tm5 using the GBV-B strand-specific PCR assay and found that the negative-strand viral RNAs were detected in the liver, spleen and PBMC samples (Fig. 4B). No negative-strand or replicating forms of the virus were detected from RNA extracted from pancreas, stomach and HeLa cells.

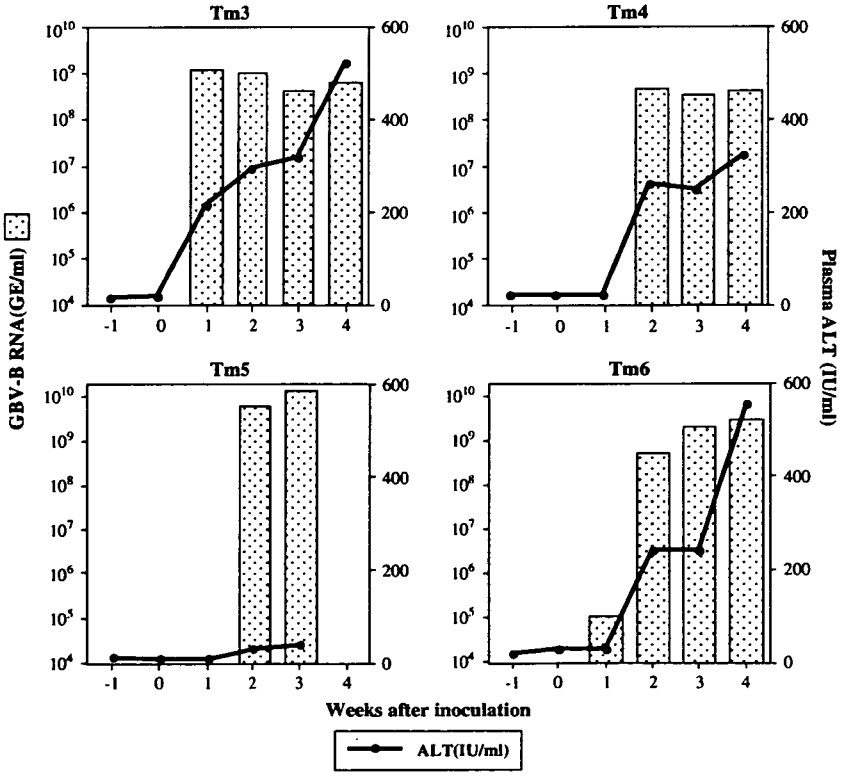


Fig. 2. Acute course of GBV-B infection in tamarins (Tm3 and Tm4) by *in vivo* passage of plasma ($7.9 \times 10^8$ GE/head) obtained from the GBV-B RNA-inoculated Tm1 in comparison with GBV-B RNA transcript-inoculated tamarins (Tm5 and Tm6). The viral RNA copies and ALT levels in the plasma samples collected from each tamarin were indicated.

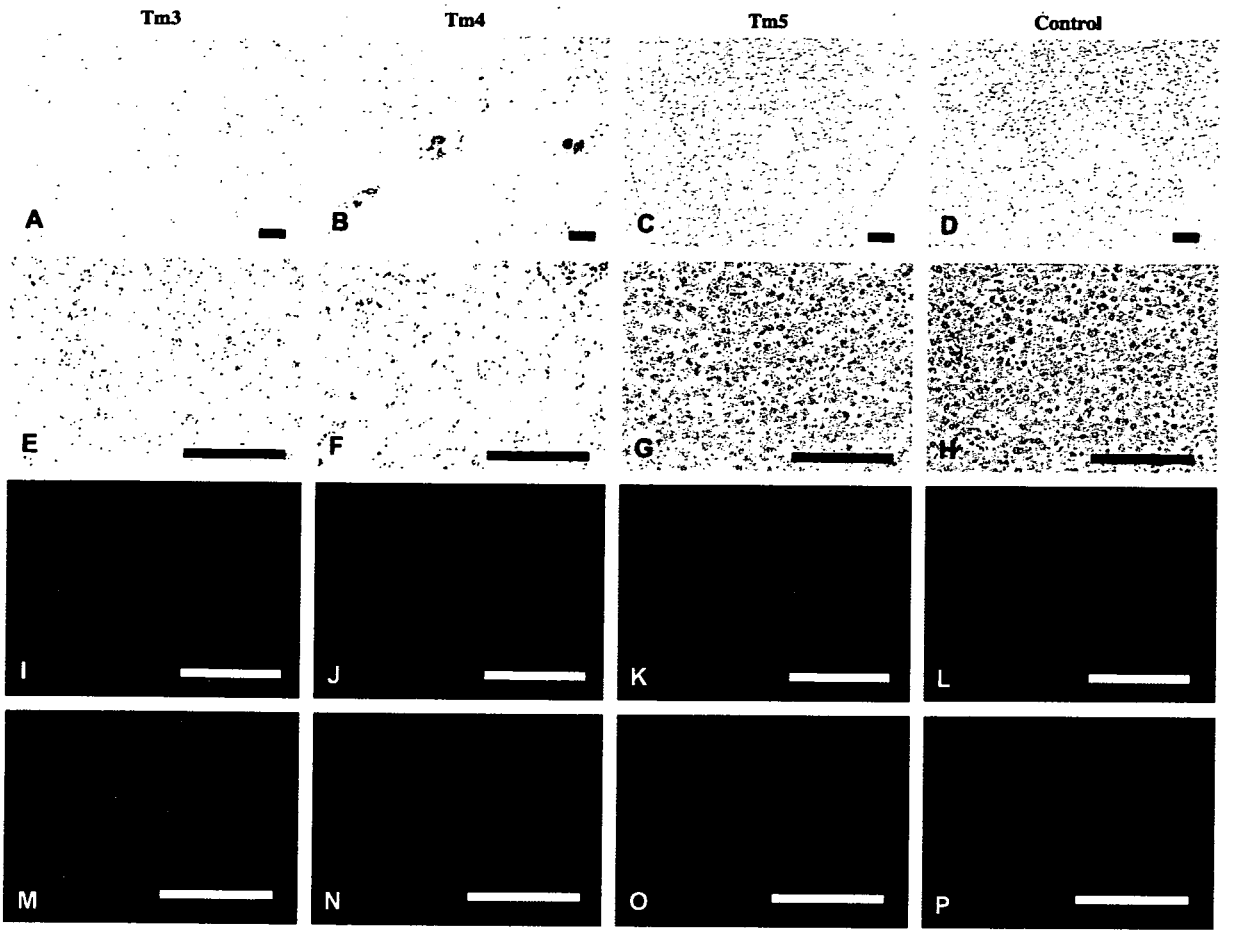


Fig. 3. Photomicrographs of liver sections from Tm3 (A, E, I, M), Tm4 (B, F, J, N), Tm5 (C, G, K, O), and an uninfected tamarin (D, H, L, P). A–H show sections with H&E staining, while I–L and M–P indicate sections with a TUNEL assay and immunohistochemistry for an active form of caspase-3, respectively. Sections immunostained for an active form of caspase-3 (green fluorescent) were counterstained with DAPI (blue fluorescent). Scale bars: 100 μm.

## 4. Discussion

GBV-B is most closely related to HCV and induces acute resolving hepatitis in tamarins. It is therefore reasonable that GBV-B has been considered to be a hepatotropic virus; in this study, however, we show for the first time that GBV-B is a pleiotropic virus and can disseminate to not only liver but also a variety of extrahepatic tissues such as hematolymphoid and genital tissues. Of note, there is ample evidence that persistent HCV infection manifests a variety of extrahepatic diseases, at least in part due to the extrahepatic tropisms of HCV (for review see [1]). This also suggests that extrahepatic tissues may serve as alternative reservoirs for HCV, while further analyses should still be required to understand the viral dynamics *in vivo*. Considering the similar pleiotropism of HCV and GBV-B, our results support and extend the usefulness of New World primates infected with GBV-B as a surrogate model for the study of pathogenesis and tropism of HCV infection.

Tamarins infected with GBV-B generally develop semi-acute viremia, of which peak levels regularly ranged from $10^7$ to $10^9$ GE/ml on the basis of previous reports [2,5,6, 14,15]. From this point of view, the peal viremia ($1.3 \times 10^{10}$ GE/ml) in Tm5 euthanized at the acute phase of the viral infection appeared to be much greater than other cases. It seems likely that in Tm5 the lymphoid tissues but not liver were responsible for the highly efficient viral production, because (i)

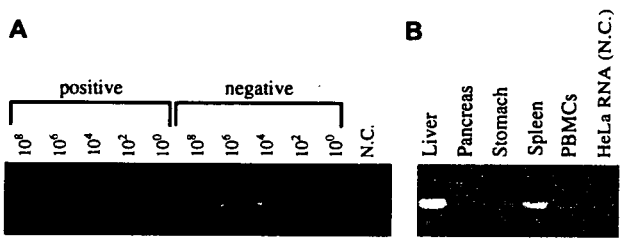


Fig. 4. (A) Titration of synthetic GBV-B RNA transcripts. Synthetic RNA transcripts corresponding to the positive- and negative-strands of part of the GBV-B were serially diluted and each transcript was subjected to amplification using strand-specific RT–PCR to determine the specificity and sensitivity of the assays. (B) Detection of negative-strand GBV-B RNA from various tissues. One microgram of total RNA obtained from tissues or cells was subjected to RT–PCR.

viral titer in the liver was lowest among three monkeys, which was consistent with minimal plasma ALT level and liver damage; (ii) yet, Tm5 exhibited highest viremia levels, (iii) the viral RNA levels in PBMCs, spleen and inguinal and intestinal lymph nodes of Tm5 were much greater than others, and (iv) we could detect negative-strand GBV-B RNA from not only liver but also spleen and PBMCs. Supposing that the entire virus in Tm3 plasma ($3.8 \times 10^8$ GE/ml) was produced in the liver of which RNA titer was highest among tamarins, most of the virus in Tm5 plasma ($1.3 \times 10^{10}$ GE/ml) should be derived from extrahepatic tissues. Taken together, our data demonstrate preferential dissemination of GBV-B in extrahepatic tissues. In order to further define the cell type(s) in which GBV-B replicates efficiently, *in situ* histological analysis should be needed as indicated in the case of HCV [16].

It was possible that differential lymphotropism among GBV-B-infected tamarins could be due to adaptive mutation in the viral genome. From this point of view, we cloned the viral RNA obtained from plasma and liver; however, we did not find any sequence heterogeneity in the viral genome (data not shown). Furthermore, challenge of Tm5 plasma to naïve tamarins developed typical semi-acute hepatitis with regular viremia and did not reproduce the preferential lymphotropism (data not shown). These results indicate that GBV-B intrinsically has pleiotropism in a host-dependent manner. It is possible that multiple surface molecules in the host cells, which act as alternative receptors, would determine the pleiotropism of GBV-B. It remains to be investigated whether host molecules which are used as receptors for HCV [17] would also be used by GBV-B.

Histopathological studies showed the inflammatory responses in Tm3 and Tm4 livers; especially, the Tm4 liver developed strong degenerative changes, which was consistent with high ALT levels (Fig. 2G,H). Furthermore, the livers of Tm3 and Tm4 showed substantial proportions of apoptotic cells as revealed by greater signals of DNA fragmentation and caspase-3 activation, both of which were popular markers of apoptosis, than those in Tm5 (Fig. 3). It needs to be clarified whether such cytopathic effects could be directly induced by GBV-B infection into hepatocytes or whether effector cytotoxic T lymphocytes would be responsible for the cytopathicity.

## Acknowledgments

We are grateful to Dr. Jens Bukh for providing pGBB. We also thank Mami Matsuda, Makiko Yahata and Tetsu Shimoji for technical assistance and members of Corporation for Production and Research of Laboratory Primates for the handling and care of the monkeys. This work was supported by a Health and Labour Science Research Grant from the Ministry of Health, Labour, and Welfare, Japan, and from New Energy and Industrial Technology Development Organization (NEDO) of Japan.

## References

[1] V. Agnello, F.G. De Rosa, Extrahepatic disease manifestations of HCV infection, J. Hepatol. 40 (2004) 341–352.
[2] J. Bukh, C.L. Apgar, M. Yanagi, Toward a surrogate model for hepatitis C virus: An infectious molecular clone of the GB virus-B hepatitis agent, Virology 262 (1999) 470–478.
[3] A.S. Muerhoff, et al., Genomic organization of GB viruses A and B: two members of the Flaviviridae associated with GB agent hepatitis, J. Virol. 69 (1996) 5621–5630.
[4] J.N. Simons, et al., Identification of two flavivirus-like genomes in the GB hepatitis agent, Proc. Natl. Acad. Sci. USA. 92 (1995) 3401–3405.
[5] A. Martin, F. Bodola, D.V. Sangar, K. Goettge, V. Popov, R. Rijnbrand, R.E. Lanford, S.M. Lemon, Chronic hepatitis associated with GB virus B persistence in a tamarin after intrahepatic inoculation of synthetic viral RNA, Proc. Natl. Acad. Sci. USA. 100 (2003) 9962–99627.
[6] J.H. Nam, K. Faulk, R.E. Engle, S. Govindarajan, M. St Claire, J. Bukh, In vivo analysis of the 3′ untranslated region of GB virus B after in vitro mutagenesis of an infectious cDNA clone: persistent infection in a transfected tamarin, J. Virol. 78 (2004) 9389–9399.
[7] J.R. Jacob, K.C. Lin, B.C. Tennant, K.G. Mansfield, GB virus B infection of the common marmoset (*Callithrix jacchus*) and associated liver pathology, J. Gen. Virol. 85 (2004) 2525–2533.
[8] B. Beames, D. Chavez, B. Guerra, L. Notvall, K.M. Brasky, R.E. Lanford, Development of a primary tamarin hepatocyte culture system for GB virus-B: a surrogate model for hepatitis C virus, J. Virol. 74 (2000) 11764–11772.
[9] T.J. Pilot-Matias, A.S. Muerhoff, J.N. Simons, T.P. Leary, S.L. Buijk, M.L. Chalmers, J.C. Erker, G.J. Dawson, S.M. Desai, I.K. Mushahwar, Identification of antigenic regions in the GB hepatitis viruses GBV-A, GBV-B, and GBV-C, J. Med. Virol. 48 (1996) 329–338.
[10] K. Tsukiyama-Kohara, N. Iizuka, M. Kohara, A. Nomoto, Internal ribosome entry site within hepatitis C virus RNA, J. Virol. 66 (1992) 1476–1483.
[11] R.L. Chaves, J. Graff, A. Normann, B. Flehmig, Specific detection of minus strand hepatitis A virus RNA by Tail-PCR following reverse transcription, Nucleic Acids Res. 22 (1994) 1919–1920.
[12] J. Mellor, G. Haydon, C. Blair, W. Livingstone, P. and Simmonds, Low level or absent in vivo replication of hepatitis C virus and hepatitis G virus/GB virus C in peripheral blood mononuclear cells, J. Gen. Virol. 79 (1998) 705–714.
[13] H. Akari, S. Bour, S. Kao, A. Adachi, K. Strebel, The human immunodeficiency virus type 1 accessory protein Vpu induces apoptosis by suppressing the nuclear factor kappaB-dependent expression of antiapoptotic factors, J. Exp. Med. 194 (2001) 1299–1311.
[14] A. Sbardellati, E. Scarselli, E. Verschoor, A. De Tomassi, D. Lazzaro, C. Traboni, Generation of infectious and transmissible virions from a GB virus B full-length consensus clone in tamarins, J. Gen. Virol. 82 (2001) 2437–2448.
[15] R.E. Lanford, D. Chavez, L. Notvall, K.M. Brasky, Comparison of tamarins and marmosets as hosts for GBV-B infections and the effect of immunosuppression on duration of viremia, Virology 311 (2003) 72–80.
[16] E.J. Gowans, Distribution of markers of hepatitis C virus infection throughout the body, Semin. Liver Dis. 20 (2000) 85–102.
[17] L. Cocquerel, C. Voisset, J. Dubuisson, Hepatitis C virus entry: potential receptors and their biological functions, J. Gen. Virol. 87 (2006) 1075–1084.

Arch Virol (2007) 152: 1019–1025
DOI 10.1007/s00705-006-0924-7
Printed in the Netherlands

Archives of Virology

*Brief Report*

# Enhancement of cytotoxicity against Vero E6 cells persistently infected with SARS-CoV by *Mycoplasma fermentans*

**T. Mizutani[1], S. Fukushi[1], T. Kenri[2], Y. Sasaki[2], K. Ishii[3], D. Endoh[5], A. Zamoto[4], M. Saijo[1], I. Kurane[1], and S. Morikawa[1]**

[1] Department of Virology 1, National Institute of Infectious Diseases, Tokyo, Japan
[2] Department of Bacteriology 2, National Institute of Infectious Diseases, Tokyo, Japan
[3] Department of Virology 2, National Institute of Infectious Diseases, Tokyo, Japan
[4] Division of Experimental Animal Research, National Institute of Infectious Diseases, Tokyo, Japan
[5] Laboratory of Veterinary Radiology, School of Veterinary Medicine, Rakuno Gakuen University, Ebetsu, Japan

Received June 15, 2006; accepted December 13, 2006; published online February 7, 2007


**Summary**

We previously reported that cells with persistent severe acute respiratory syndrome coronavirus (SARS-CoV) infection were established after apoptotic events. In the present study, we investigated the cytopathic effects of dual infection with SARS-CoV and *Mycoplasma fermentans* on Vero E6 cells. Dual infection completely killed cells and prevented the establishment of persistent SARS-CoV infection. *M. fermentans* induced inhibition of cell proliferation, but the cells remained alive. Apoptosis was induced easily in *M. fermentans*-infected cells, indicating that they were primed for apoptosis. These results indicated that *M. fermentans* enhances apoptosis in surviving cells that have escaped from SARS-CoV-induced apoptosis.

Author's address: Dr. Tetsuya Mizutani, Department of Virology 1, National Institute of Infectious Diseases, Gakuen 4-7-1, Musashimurayama, Tokyo 208-0011, Japan.
e-mail: tmizutan@nih.go.jp

*

Severe acute respiratory syndrome (SARS) is a newly discovered infectious disease caused by SARS coronavirus (SARS-CoV), which became a global health threat due to its rapid transmission and high fatality rate [10, 20]. Vero E6 is a cell line derived from African green monkey kidney cells and is sensitive to SARS-CoV. SARS-CoV induces apoptosis into Vero E6 cells *via* activation of caspase-3 [14]. Activation of p38 mitogen-activated protein kinase (MAPK) induces cell death [14] and inactivation of Akt induces apoptosis [15]. In virus-infected cells, c-Jun N-terminal protein kinase (JNK), extracellular signal-related kinase (ERK)1/2, and 90-kDa ribosomal S6 kinases are also phosphorylated [13, 17]. Four groups, including our groups, independently reported that a small population of virus-infected cells remained alive after the

majority of virus-infected cells had died, and these cells grew with virus production [3, 16, 19, 24].

There have been reports of patients who were dual-infected with SARS-CoV and *Chlamydia pneumoniae*, *Mycoplasma pneumoniae*, or human metapneumovirus [2, 5, 9, 25]. However, the clinical significance of viral or bacterial co-infection with SARS in patients is still unclear. In the present study, we investigated cytopathic effects of *M. fermentans* on Vero E6 cells, and we investigated the cytotoxicity of dual infection with SARS-CoV and *M. fermentans* in Vero E6 cells. *M. fermentans* is known to enhance human immunodeficiency virus (HIV) replication [1]. Activation of NFκB by infection with *M. fermentans* increased replication of HIV by regulation of the long terminal repeat (LTR) [21, 23]. Thus, it is possible that *M. fermentans* can influence pathogenesis in co-infection with other viruses. *M. fermentans* is detected in approximately 10% of HIV-seronegative individuals [8], suggesting that a certain percentage of the healthy population is infected with *M. fermentans*. The present study was performed to examine whether pathogenicity is increased by co-infection with *M. fermentans* and SARS-CoV using an *in vitro* cell culture system.

Vero E6 cells were cultured in Dulbecco's modified Eagle's medium (DMEM; Sigma, St. Louis, MO, USA) supplemented with 0.2 mM L-glutamine, 100 units/ml penicillin, 100 μg/ml streptomycin, and 5% (v/v) fetal bovine serum (FBS), and maintained at 37 °C in an atmosphere of 5% $CO_2$. In the present study, Vero E6 cells were treated at least three times with MC-210 (Dainippon Sumitomo Pharma Co. Ltd., Osaka, Japan), which is an antibiotic active against mycoplasma. After washing MC-210 from the medium, mycoplasma contamination was checked, and the cells were confirmed to be mycoplasma-free by incubation in glucose-containing PPLO medium. SARS-CoV, which was isolated as Frankfurt 1 and kindly provided by Dr. J. Ziebuhr, was used in the present study. Mycoplasma broth medium consisted of PPLO broth (Difco Laboratories, Franklin Lakes, NJ, USA), yeast extract (Difco), 15% heat-inactivated horse serum, 10% aqueous glucose, and 1000 units/ml penicillin as described previously [7]. In the present study, we used the *M. fermentans* M64 strain, which was isolated from a patient with acute respiratory disease. *M. fermentans* was grown aerobically in glucose-containing PPLO medium at 30 °C for 24 h, and then frozen at −80 °C.

Aliquots of $5 \times 10^7$ colony-forming units (CFU) of *M. fermentans* in 250 μl of glucose-containing PPLO medium were added to approximately $2 \times 10^6$ Vero E6 cells (100% confluency) in 1 ml of 5%-FBS-containing DMEM in 24-well plates. Mock-infected cultures were prepared with 250 μl of glucose-containing PPLO medium. After 24 h, the cells were infected with SARS-CoV at 2 m.o.i., and the cells were fixed and stained 7 days after virus infection. As shown in Fig. 1A, both *M. fermentans*- and mock-infected cells maintained confluency. No significant morphological changes were observed in the *M. fermentans*- or mock-infected cells when confluent cells were infected. The majority of SARS-CoV-infected cells died by apoptosis at 48 h.p.i., and persistently infected cells were observed at 7 days p.i. (Fig. 1A). Our recent studies indicated that these persistently infected cells grow well and produce viral particles in the medium [16]. On the other hand, all cells died 7 days after dual infection with *M. fermentans* and SARS-CoV. The observation in Fig. 1A raised questions regarding the stage at which *M. fermentans* kills cells that have escaped from apoptosis by SARS-CoV infection. We next examined the effects of *M. fermentans* infection at the late stages of SARS-CoV infection on cells persistently infected with SARS-CoV. Vero E6 cells were infected with SARS-CoV, and almost all cells died by apoptosis at 50 h.p.i. However, a small population of cells survived. At this time point, the cells were infected with *M. fermentans*. The cells were fixed and stained 8 days after SARS-CoV infection. As shown in Fig. 1B, persistently SARS-CoV-infected cells were not observed with additional *M. fermentans* infection. These results indicated that *M. fermentans* killed all surviving cells that had escaped from SARS-CoV-induced apoptosis and prevented the establishment of persistent SARS-CoV infection.

We investigated whether *M. fermentans* shows cytopathic effects on subconfluent Vero E6 cells. Approximately 5000 cells in 96-well plates were

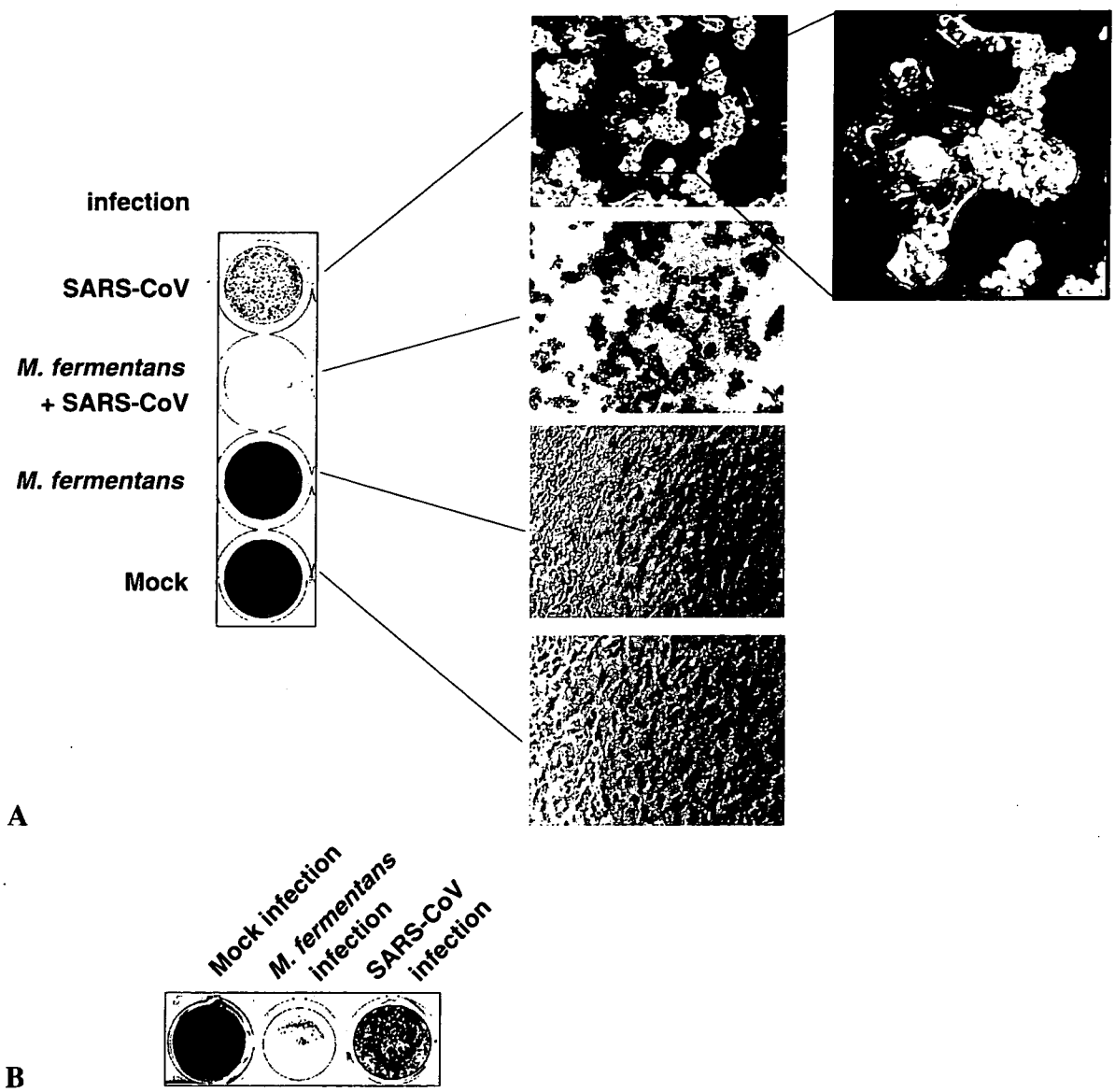


**Fig. 1.** Enhancement of cytotoxicity by dual infection with SARS-CoV and *M. fermentans*. **A** Confluent Vero E6 cells in 24-well plates were infected with 100 CFU/cell of *M. fermentans* for 24 h, and then the cells were infected with SARS-CoV at 2 m.o.i. A 20% volume of glucose-containing PPLO medium was added to all wells. After incubation for 7 days, surviving cells were observed in SARS-CoV-infected cultures, but not in dual-infected cultures. The cells were fixed with 10% formaldehyde for at least 24 h and stained with 0.1% naphthol blue black for 30 min. After washing with water, the plates were scanned using a GT-9400UF scanner (Epson, Tokyo, Japan). **B** Confluent Vero E6 cells were infected with SARS-CoV for 50 h, and then the cells were infected with *M. fermentans*. The cells were fixed and stained

inoculated with $5 \times 10^6$ CFU of *M. fermentans*. The results shown in Fig. 2A indicate that morphological changes in *M. fermentans*-infected cells were observed after day 1. The cells adopted an angular shape following infection with *M. fermentans*. As shown in Fig. 2B, cell growth was suppressed in the *M. fermentans*-infected cells. To clarify why cell proliferation is inhibited in *M. fermentans*-infected cells, Western blot analysis was performed using anti-retinoblastoma (Rb) antibody. Rb is thought

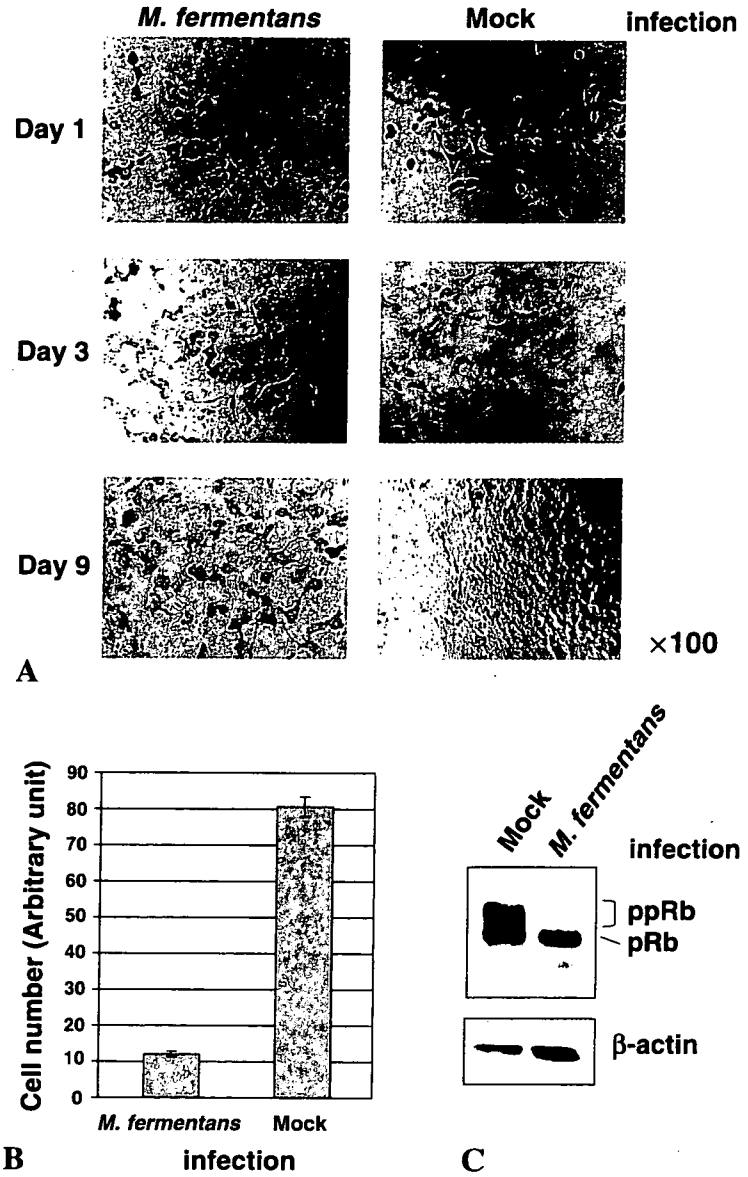


**Fig. 2.** Inhibition of cell proliferation by *M. fermentans* infection. **A** Subconfluent Vero E6 cells were infected with *M. fermentans* for 1, 3, and 9 days. **B** The cells at 9 days were fixed and stained. Cells were counted using a convenient method described by Everitt and Wohlfart for determination of the actual or relative number of cells in anchorage culture [4]. The dye-protein complexes were released hydrolytically with 0.1 M NaOH and measured spectrophotometrically at 660 nm. **C** Western blot analysis was performed using cell lysate 2 days after infection. Mouse anti-retinoblastoma protein (Rb) monoclonal antibody, which is able to detect the underphosphorylated form (pRb) and hyperphosphorylated from (ppRb), was purchased from BD Biosciences (Franklin Lakes, NJ, USA) and used at a dilution of 1:500. Mouse anti-β-actin antibody was purchased from Sigma and used at a dilution of 1:5000

to play one of key roles in the regulation of the G1 > S phase transition in the cell cycle, and phosphorylation of Rb is an important event in progression at G1 > S [18]. Only the hypophosphorylated form of pRb was detected in *M. fermentans*-infected cells at 2 days (Fig. 2C). The hypophosphorylated form of pRb is largely found in the early G1 phase.

Next, we examined the susceptibility of subconfluent *M. fermentans*-infected cells to apoptosis. Subconfluent cells were infected with *M. fermentans* for 24 h, and cycloheximide (final concentration, 1 mM) was added to the cells to stimulate apoptosis. As the cycloheximide was dissolved in DMSO, the same volume of DMSO alone was added to experimental controls. The subconfluent cells were infected with *M. fermentans* for 21 h, and cycloheximide or DMSO was added to the cells for 2 h. The cells were treated for 30 min with Apopercentage (Biocolor Ltd., Newtownabbey, Northern Ireland), which stains apoptotic cells at the early time stages by changing their color to red, and then the medium was replaced by PBS. As shown in Fig. 3A, the color of *M. fermentans*-infected cells treated with

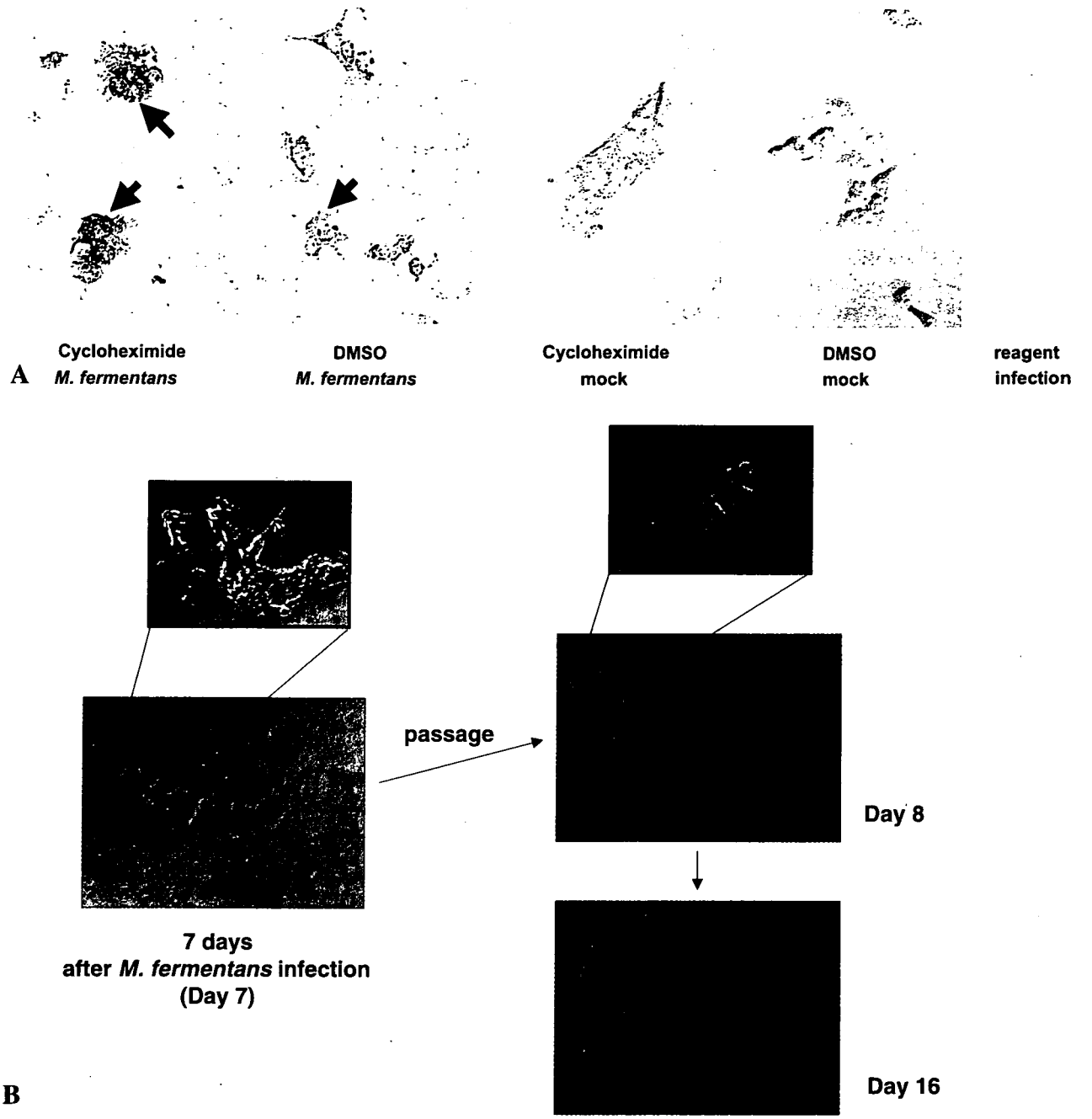


**Fig. 3.** Viability of *M. fermentans*-infected cells. **A** Subconfluent cells were infected with *M. fermentans* for 21 h, and then the cells were treated with cycloheximide. Apopercentage was used for detection of apoptosis. The arrows indicate apoptotic cells. **B** After 7 days postinfection, cells were passaged and cultured for 1 and 9 days

cycloheximide changed to red, indicating apoptosis, whereas mock-infected cells showed no change in color. However, some DMSO-treated cells infected with *M. fermentans* also changed color to red, but DMSO-treated cells without infection did not, suggesting that stimulation with not only cycloheximide but also DMSO induced apoptosis of *M. fermentans*-infected cells. Therefore, this result

indicated that *M. fermentans*-infected cells were primed for apoptosis. It remained to be determined whether *M. fermentans*-infected cells were alive. Therefore, subconfluent *M. fermentans*-infected cells at 7 days were trypsinized and resuspended in 5%-FBS-containing DMEM with MC-210 to kill the mycoplasma. After one day, almost all cells were attached to the plate, and dividing cells were observed (Fig. 3B). This result indicated that the *M. fermentans*-infected cells were alive and were able to grow when *M. fermentans* was removed.

In the present study, we demonstrated enhancement of cytotoxicity against Vero E6 cells persistently infected with SARS-CoV by *M. fermentans*. As *M. fermentans* processes phospholipase C in the cell membrane [22], the morphological changes caused by infection of Vero E6 cells with *M. fermentans* may be due to partial destruction of cell-surface lipids. In addition, cell death by superinfection of persistently SARS-CoV-infected cells with *M. fermentans* may be induced by phosphorylated p38 MAPK [12, 14], and assembly of the SARS-CoV envelope on the cell surface in surviving cells may also be a trigger of cell death on infection with *M. fermentans*. Akt, JNK, Bcl-2 and Bcl-xL play important roles in the establishment of SARS-CoV-persistent infection [12], and nucleocapsid (N) protein of SARS-CoV using a vaccinia virus expression system [6] is able to induce phosphorylation of Akt and JNK, but not p38 MAPK [12]. Glycogen synthase kinase 3β, which is downstream of Akt, was phosphorylated in N-expressing cells (data not shown). These results suggested that the N protein plays important roles for preventing apoptosis. On the other hand, Vero E6 cells were primed for apoptosis by *M. fermentans* infection in our experimental system, but cell death was not induced by infection. As infection by an excess of *M. fermentans* more than used in this study sometimes kills subconfluent Vero E6 cells, *M. fermentans* itself may be able to kill Vero E6 cells. Therefore, when the number of surviving cells that have escaped from cell death by SARS-CoV infection is very low, it is thought that cell death is enhanced by apoptotic effects of both SARS-CoV and *M. fermentans* infection.

The results of this study demonstrate that cells stressed by infection with *M. fermentans* are subject to further stress after infection with SARS-CoV. This phenomenon is important for understanding clinical pathogenicity, because it is unlikely that patients will be infected with only a single pathogen. There have been no previous reports regarding the pathological implications of dual infection with SARS-CoV and viruses or bacteria using a cell culture system. The findings of the present study have implications for infection control of acute or persistent SARS. Dual infection of the kidney cell line Vero E6 with SARS-CoV and *M. fermentans* also provides important information to further our understanding of renal infection in SARS patients.

## Acknowledgments

We thank Dr. S. Harada (National Institute of Infectious Diseases, Japan) for helpful suggestions. We also thank Ms. M. Ogata (National Institute of Infectious Diseases, Japan) for her assistance. This work was supported in part by the Japan Health Science Foundation and, Japan Society for Promotion of Science, Tokyo, Japan.

## References

1. Bauer FA, Wear DJ, Angritt P, Lo SC (1991) *Mycoplasma fermentans* (incognitus strain) infection in the kidneys of patients with acquired immunodeficiency syndrome and associated nephropathy: a light microscopic, immunohistochemical, and ultrastructural study. Hum Pathol 22: 63–69
2. Chan PK, Tam JS, Lam CW, Chan E, Wu A, Li CK, Buckley TA, Ng KC, Joynt GM, Cheng FW (2003) Human metapneumovirus detection in patients with severe acute respiratory syndrome. Emerg Infect Dis 9: 1058–1063
3. Chan PK, To KF, Lo AW, Cheung JL, Chu I, Au FW, Tong JH, Tam JS, Sung JJJ, Ng HK (2004) Persistent infection of SARS coronavirus in colonic cells in vitro. J Med Virol 74: 1–7
4. Everitt E, Wohlfart C (1987) Spectrophotometric quantitation of anchorage-dependent cell numbers using extraction of naphthol blue-black-stained cellular protein. Anal Biochem 162: 122–129
5. Hong T, Wang JW, Sun YL, Duan SM, Chen LB, Qu JG et al. (2003) Chlamydia-like and coronavirus-like agents found in dead cases of atypical pneumonia by electron microscopy. Zhonghua Yi Xue Za Zhi 83: 632–636

6. Ishii K, Hasegawa H, Nagata N, Mizutani T, Morikawa S, Suzuki T, Taguchi F, Tashiro M, Takemori T, Miyamura T, Tsunetsugu-Yokota Y (2007) Induction of protective immunity against severe acute respiratory syndrome coronavirus (SARS-CoV) infection using highly attenuated recombinant vaccinia virus DIs. Virology (in press)
7. Kenri T, Seto S, Horino A, Sasaki Y, Sasaki T, Miyata M (2004) Use of fluorescent-protein tagging to determine the subcellular localization of mycoplasma pneumoniae proteins encoded by the cytadherence regulatory locus. J Bacteriol 186: 6944–6955
8. Kovacic R, Launay V, Tuppin P, Lafeuillade A, Feuillie V, Montagnier L, Grau O (1996) Rsearch for the presence of six Mycoplasma species in peripheral blood mononuclear cells of subjects seropositive and seronegative for human immunodeficiency virus. J Clin Microbiol 34: 1808–1810
9. Kuiken T, Fouchier RA, Schutten M, Rimmelzwaan GF, van Amerongen G, van Riel D, Laman JD, de Jong T, van Doornum G, Lim W et al. (2003) Newly discovered coronavirus as the primary cause of severe acute respiratory syndrome. Lancet 362: 263–270
10. Marra MA, Jones SJM, Astell CR, Holt RA, Brooks-Wilson A, Butterfield YSN, Khattra J, Asano JK, Barber SA, Chan SY et al. (2003) The genome sequence of the SARSassociated coronavirus. Science 300: 1399–1404
11. Mizutani T, Fukushi S, Iizuka D, Inanami O, Kuwabara M, Takashima H, Yanagawa H, Saijo M, Kurane I, Morikawa S (2006) Inhibition of cell proliferation by SARS-CoV infection in Vero E6 cells. FEMS Immunol Microbiol 46: 236–243
12. Mizutani T, Fukushi S, Ishii K, Sasaki Y, Kenri T, Saijo M, Kanaji Y, Shirota K, Kurane I, Morikawa S (2006) Mechanisms of establishment of persistent SARS-CoV-infected cells. Biochem Biophys Res Commun 347: 261–265
13. Mizutani T, Fukushi S, Murakami M, Hirano T, Saijo M, Kurane I, Morikawa S (2004) Tyrosine dephosphorylation of STAT3 in SARS coronavirus-infected Vero E6 cells. FEBS Lett 577: 187–192
14. Mizutani T, Fukushi S, Saijo M, Kurane I, Morikawa S (2004) Phosphorylation of p38 MAPK and its downstream targets in SARS coronavirus-infected cells. Biochem Biophys Res Commun 319: 1228–1234
15. Mizutani T, Fukushi S, Saijo M, Kurane I, Morikawa S (2004) Importance of Akt signaling pathway for apoptosis in SARS-CoV-infected Vero E6 cells. Virology 327: 169–174
16. Mizutani T, Fukushi S, Saijo M, Kurane I, Morikawa S (2005) JNK and PI3k/Akt signaling pathways are required for establishing persistent SARS-CoV infection in Vero E6 cells. Biochem Biophys Acta 1741: 4–10
17. Mizutani T, Fukushi S, Saijo M, Kurane I, Morikawa S (2006) Regulation of p90RSK phosphorylation by SARS-CoV infection in Vero E6 cells. FEBS Lett 580: 1417–1424
18. Nevins JR, Leone G, DeGregori J, Jakoi L (1997) Role of the Rb/E2F pathway in cell growth control. J Cell Physiol 173: 233–236
19. Palacios G, Jabado O, Renwick N, Briese T, Lipkin WI (2005) Severe acute respiratory syndrome coronavirus persistence in Vero cells. Chin Med J (Engl) 118: 451–459
20. Rota PA, Oberste MS, Monroe SS, Nix WA, Campagnoli R, Icenogle JP, Penaranda S, Bankamp B, Maher K, Chen MH et al. (2003) Characterization of a novel coronavirus associated with severe acute respiratory syndrome. Science 300: 1394–1399
21. Sasaki Y, Honda M, Makino M, Sasaki T (1993) Mycoplasmas stimulate replication of human immunodeficiency virus type 1 through selective activation of $CD^{4+}$ T lymphocytes. AIDS Res Hum Retrovir 9: 775–780
22. Shibata K, Sasaki T, Watanabe T (1995) AIDS-associated mycoplasmas possess phospholipases C in the membrane. Infect Immunol 63: 4174–4177
23. Shimizu T, Kida Y, Kuwano K (2004) Lipid-associated membrane proteins of Mycoplasma fermentans and M. penetrans activate human immunodeficiency virus long-terminal repeats through Toll-like receptors. Immunology 113: 121–129
24. Yamate M, Yamashita M, Goto T, Tsuji S, Li YG, Warachit J, Yunoki M, Ikuta K (2005) Establishment of Vero E6 cell clones persistently infected with severe acute respiratory syndrome coronavirus. Microbes Infect 7: 1530–1540
25. Zahariadis G, Latchford MI, Ryall P, Hutchinson C, Fearon M, Jamieson F et al. (2003) Incidence of respiratory pathogens in patients with fever and respiratory symptoms during a SARS epidemic. In: Abstracts of the 43rd Infectious Disease Society of America Conference, San Diego, California, October 7–13, Abstract no. LB-16